Title	Elevated blood pressure aggravates intracerebral hemorrhage-induced brain injury
Author(s)	Sang, YH; Su, HX; Wu, WT; So, KF; Cheung, RTF
Citation	Journal Of Neurotrauma, 2011, v. 28 n. 12, p. 2523-2534
Issued Date	2011
URL	http://hdl.handle.net/10722/149774
Rights	This is a copy of an article published in the Journal of Neurotrauma © 2011 copyright Mary Ann Liebert, Inc.; Journal of Neurotrauma is available online at: http://www.liebertonline.com.

JOURNAL OF NEUROTRAUMA 28:2523–2534 (December 2011)

DOI: 10.1089/neu.2010.1680

Elevated Blood Pressure Aggravates Intracerebral Hemorrhage-Induced Brain Injury

Yan-Hua Sang,[1,2] Huan-Xing Su,[2] Wu-Tian Wu,[2,3] Kwok-Fai So,[2,4] and Raymond Tak-Fai Cheung[1,4]

Abstract

Elevated blood pressure (BP) is commonly seen in patients with intracerebral hemorrhage (ICH), and is independently associated with poor functional outcomes. Little is known about how elevated BP influences ICH-related brain injury. In the present study, we investigated the physiological and brain histological changes, as well as functional recovery following ICH in renovascular hypertensive rats. Renovascular hypertension (RVHT) was achieved by applying a silver clip onto the left renal artery of adult Sprague-Dawley rats. ICH was induced by an intrastriatal injection of bacterial collagenase IV about 5–6 weeks after left renal artery clipping or the sham operation. Following induction of ICH, both the normotensive and RVHT rats demonstrated an ultra-acute elevation in BP. Elevated BP increased hematoma volume, brain swelling, and apoptosis in the perihematomal areas. Brain degeneration, including local atrophy and lateral ventricle enlargement, was greater in the RVHT rats. In addition, many proliferating cells were seen over the ipsilateral striatum in the RVHT rats after ICH. The modified limb placing tests were done weekly for 3 weeks. In line with the histological damage, elevated BP worsened neurological deficits. These results suggest that ICH in the hypertensive rats mimics the clinical scenario of hypertensive ICH and may provide a platform to study the mechanisms of ICH-induced brain injury and potential therapies for ICH.

Key words: cell proliferation; functional deficits; hypertension; intracerebral hemorrhage

Introduction

Intracerebral hemorrhage (ICH) accounts for 10 to 15% of all strokes and has the highest mortality rate (Broderick et al., 2007; Caplan, 1992). Only 20% of patients are independent at 6 months after ICH (Gebel and Broderick, 2000). Hypertension is the most important risk factor for ICH (Brott et al., 1986). The most common site of hypertensive ICH is the striatum. Recent clinical evidence suggests that elevated blood pressure (BP), as defined by BP $\geq$140/90 mmHg, is seen in more than 70% of patients in the acute period of ICH (Qureshi et al., 2007). Elevated BP may contribute to ICH and is associated with poor outcomes (Qureshi, 2008; Vemmos et al., 2004). To optimize BP management in ICH patients, it is necessary to understand the direct effects of elevated BP on ICH-induced brain injury.

Several animal models of hypertension are available (Leenen and de Jong, 1971; Okamoto et al., 1986; Zeng et al., 1998). The 2-kidney, 1-clip (2K1C) model, introduced by Wilson and Byromv (1939), is widely accepted. In the 2K1C model, a silver clip is applied on a renal artery, leaving the contralateral artery undisturbed. This has a high yield of hypertensive animals, and renin-angiotensin system (RAS) is involved in the hypertensive process (DeForrest et al., 1982). Circulating levels of renin and aldosterone rise in the early phase of hypertension and return to normal when hypertension is moderate with systolic BP $<$200 mmHg (Brunner et al., 1971; Koletsky et al., 1971). The systemic level of angiotensin II (Ang II) follows a similar pattern (Lerman et al., 2005).

Previous studies have demonstrated the chronic hypertension-induced brain damage (Al-Sarraf and Philip, 2003; Wakisaka et al., 2008). However, there is little experimental data concerning the direct effect of elevated BP on ICH-related brain injury (Gonzalez-Darder and Duran-Cabral, 1990). In the present study, we investigated the effects of elevated BP on the physiological parameters, acute brain injury and delayed brain degeneration, proliferation of endogenous neural stem cells (NSCs), and functional recovery in a rat ICH model.

Methods

Animals

Experimental protocols were approved by the Committee on the Use of Live Animals in Teaching and Research, the

[1]Department of Medicine, [2]Department of Anatomy, [3]Research Center of Reproduction, Development and Growth, [4]Research Centre of Heart, Brain, Hormone and Healthy Aging, Li Ka Shing Faculty of Medicine, The University of Hong Kong, China.

University of Hong Kong. Standard chow-fed adult male Sprague-Dawley rats, weighing between 260 and 280 g, were obtained from the Laboratory Animal Unit, the University of Hong Kong. Rats were maintained under diurnal lighting conditions with free access to food and water for about 4 days before experimentation. All surgical procedures were performed with aseptic techniques. The rats were randomly allocated to one of the two groups: the RVHT group and normotensive group. A total of 42 rats were used to induce RVHT, of which seven rats were excluded because of failure in achieving elevated BP 5 weeks after renal artery clipping and one was euthanized due to severe weight loss after surgery. Eleven weeks after the renal artery clipping or sham operation, the brain and kidneys were collected for histological study ($n=4$ in normotensive group and n = 8 in RVHT group). ICH was induced in 31 normotensive rats and 26 hypertensive rats. The right femoral artery was cannulated for BP measurement from 10 min before ICH to 4 h after ICH onset ($n=6$ in normotensive group and $n=5$ in RVHT group). The rats that had undergone invasive BP measurement were sacrificed for examination of their kidneys and heart. One day after ICH, some rats were sacrificed for assessment of hemoglobin content ($n=8$ in normotensive group and $n=5$ in RVHT group) and brain swelling ($n=5$ in each group). Apoptosis and new cell proliferation in the perihematomal areas 10 days after ICH were evaluated immunohistochemically ($n=5$ in each group). Twenty-one days after ICH, some rats ($n=7$ in normotensive group and $n=6$ in RVHT group) were sacrificed for measurement of the lesion volume, brain tissue loss and lateral ventricle enlargement. Neurological deficits were assessed at 1, 3, 7, 10, 14, and 21 days after ICH.

RVHT model

RVHT was induced by applying a solid silver clip onto the left renal artery, leaving the contralateral artery undisturbed (Leenen and de Jong, 1971; Zeng et al., 1998). In brief, 6- to 8-week-old male rats were anesthetized with an intraperitoneal injection of ketamine (67 mg/kg) and xylazine (6 mg/kg). After anesthesia, a 3-cm median longitudinal skin incision was made in the abdomen. The left renal artery was stretched, separated from the left renal vein. A clip with the internal diameter of 0.25 mm was applied onto the exposed left renal artery as close to the aorta as possible. Sham RVHT was achieved by the same procedure except that no clip was placed onto the left renal artery. Free access to food and water was allowed after recovery from the anesthesia.

BP measurement

Systolic BP (SBP) and body weight were measured weekly after renal artery constriction. SBP was measured by an indirect tail-cuff method (Kurtz et al., 2005). Rats were observed for 10 min daily to assess their general behavior, including grooming and exploratory activities, level of alertness, and physical well-being. Rats with SBP >150 mmHg at 5 weeks after renal artery constriction were characterized as RVHT rats for subsequent ICH study.

Histological examination of brain and kidneys

At 11 weeks of renal artery constriction or sham operation, some rats were anesthetized with an intraperitoneal injection of sodium pentobarbital (55 mg/kg) and sacrificed for histological examination by transcardial perfusion with 4% paraformaldehyde in 0.1 M phosphate buffer (PB). Coronal brain sections of 10 μm thickness were obtained from 4 mm anterior to the bregma to 10 mm posterior to the bregma and stained with hematoxylin and eosin (HE). Four micron-thick paraffin sections obtained from the kidneys were stained with periodic acid-Schiff (PAS) reagent. Slides were examined under the light microscope.

Collagenase injection-induced ICH

Experimental ICH was induced via an intrastriatal injection of type IV collagenase (Matsushita et al., 2000; Park et al., 2005). In brief, after an intraperitoneal injection of sodium pentobarbital (55 mg/kg), the rat was placed in a stereotaxic frame. A 2-mm diameter burr hole was drilled along the left coronal suture at 3.0 mm lateral to the bregma. A 30-gauge needle was inserted into the left striatum at the coordinates of 0.2 mm anterior to the bregma, 3 mm lateral to the midline, and 6 mm underneath the skull. ICH was induced by administration of 1.0 μL saline containing 0.2 U collagenase IV (Sigma-Aldrich, St. Louis, MO) over 10 min. Once the infusion was completed, the needle was left in place for 5 min. The burr hole was sealed with bone wax, and the incision was sutured. Rectal temperature was maintained at 36.5–37.5°C throughout the experiment, and the rat was kept at 37°C during recovery. Sham ICH was achieved by the same procedures except that an equal volume of saline was injected.

Femoral artery BP measurement and biometric markers

Mean arterial BP (MAP) is the perfusion pressure for organs. The left femoral artery was cannulated for continuous measurement of MAP and heart rate between 30 min before and 4 h after collagenase IV injection, and blood sample was obtained for glucose measurement. The rat was then deeply anesthetized with sodium pentobarbital (80 mg/kg) and perfused transcardially with saline, and then 4% paraformaldehyde in 0.1 M PB. The kidneys and heart were collected and weighed.

Hematoma volume

Hematoma volume was quantified at 24 h using a spectrophotometric assay (Choudhri et al., 1997; MacLellan et al., 2004; Park et al., 2005). In brief, hemispheric brain tissue discarding the olfactory bulbs and cerebellum was acquired from the rat following transcardial perfusion. The tissue was homogenized in 3 mL 0.01 M phosphate-buffered saline (PBS), and this was followed by 1 min of sonication on ice. After centrifugation at 12,000 g for 30 min, 100 μL supernatant was reacted with 400 μL Drabkin's reagent (Sigma-Aldrich) for 15 min. The absorbance reading minus background reading at 540 nm was determined with a spectrophotometer (Bio-TEK Instruments, Winooski, VT). Using a previously determined curve from known hemoglobin contents, the hematoma volume in the perfused brain was quantified.

Lesion volume, brain swelling, and volume of lost brain tissue

The rat was deeply anesthetized with sodium pentobarbital (80 mg/kg) and then transcardially perfused with saline

followed by 4% paraformaldehyde in 0.1 M PB. The brain was sliced into nine 1 mm-thick coronal slices centered at the needle entry site. Images of the brain slices were taken using a digital camera and analyzed with Image J software (NIH, Bethesda, MD) by an observer who was blinded to group identity. Lesion volume was calculated as the sum of the lesion area on each slice and multiplied by the slice thickness on day 1 and 21 days after ICH. Brain swelling was defined as follows: ipsilateral hemisphere volume minus contralateral hemisphere volume/contralateral hemisphere volume $\times 100\%$. It was measured one day after ICH. The volume of lost brain tissue 21 days after ICH was defined as the volume of the contralateral hemisphere minus volume of normal-looking tissue on the ipsilateral hemisphere (Auriat et al., 2005). The lateral ventricle volume was quantified via Image J software (NIH) 21 days after ICH or sham ICH. Lateral ventricle volume was acquired by summing the lateral ventricle area in each slice multiplied by the slice thickness. The ventricles were not included in the measurements of brain swelling and the volume of lost brain tissue.

Tissue preparation and immunohistochemical studies

The brain used for BrdU staining and TUNEL assay was processed as follows. The rat was deeply anesthetized with sodium pentobarbital (80 mg/kg) and perfused transcardially with ice-cold saline, and then 4% paraformaldehyde in 0.1 M PB for 20 min. The brain was post-fixed in 4% paraformaldehyde overnight at 4°C before placing in 30% sucrose in 0.1 M PB for 4 days. Brain sections of 30 μm were obtained between 3 mm anterior to the bregma and 4 mm posterior to the bregma using a cryostat at −18°C. Brain sections were affixed on Superfrost Plus slides (Menzel-Glaser, Braunschweig, Germany), air-dried overnight, and stored for IHC studies.

Proliferating cells were labeled with thymidine-analogue 5-bromo-2-deoxyuridine (BrdU, Sigma-Aldrich), which was given by intraperitoneal injection at 50 mg/kg twice daily from day 6 to day 9 after ICH. The rat was sacrificed on day 10. The brain sections were denatured by incubation in citrate buffer at 95°C for 30 min and then in 2 N hydrochloric acid at 37°C for 30 min. After blocking with 10% normal goat serum in PBS, the brain sections were incubated with Rat anti-BrdU (1:1000, Abcam, Cambridge, MA) overnight at room temperature. The brain sections were then rinsed and incubated with biotinylated goat anti-rat antibody (1:200, Vector, Burlingame, CA) for 2 h. Avidin-biotin complex solution was used to amplify the IHC signal, which was visualized by diaminobenzidine (DAB) as the chromogen. For negative controls, either the primary or the secondary antibody was omitted or the same staining procedures were followed.

For double fluorescent staining, the brain sections were incubated with rat anti-BrdU (1:1000, Abcam) and mouse anti-nestin (1: 200, Millipore, Billerica, MA) overnight at room temperature. Goat anti-rat secondary antibody conjugated to Alexa 488 and goat anti-mouse antibody conjugated to Alexa 568 (1:400) were applied at room temperature for 2 h. The brain sections were coverslipped with anti-fade mounting media (Dako, Hamburg, Germany). Cells double-labeled with BrdU and nestin were counted with a confocal microscope (LSM510 META, Carl Zeiss Meditec, Jena, Germany). Counts were averaged over four grids (462×425 μm each) adjacent to the hematoma.

Apoptosis

Apoptosis was assessed using terminal deoxynucleotidyl transferase dUTP nick end labeling (TUNEL) assay with an *in situ* cell death detection kit (Roche, Indianapolis, IN) (Chu et al., 2004b; Jung et al., 2004; Lee et al., 2006). The brain sections were blocked with 3% H_2O_2 in methanol to quench the endogenous horseradish peroxidase. The sections were first incubated in the permeabilization solution and then incubated in labeling reaction mixture at 37°C in the dark for 60 min. After incubating in converter-POD at 37°C for 30 min, the brain sections were stained with DAB-H_2O_2. Three brain sections per rat at 1 mm interval were analyzed under the light microscope.

Stereological analyses

Counting of TUNEL-labeled cells and BrdU positive cells were performed stereologically using an Olympus fluorescent scope with the optical fractionators method and Stereo-Investigator v.6.0 (MicroBrightField, Williston, VT). First, the contour of the ipsilateral striatum excluding the hematoma lesion core was outlined with the Stereoinvestigator program. Systemic random sampling was done within the outlined region at $200\times$ magnifications. Cells were counted within a counting box, with the cells in the upper-most focal plane being ignored to avoid oversampling errors. The total counts from the brain sections were converted to cell densities to facilitate quantification and comparison between groups.

Behavioral tests

A standardized battery of behavioral tests was used to quantify neurological function before and 1, 3, 7, 10, 14, and 21 days after ICH by an observer who was blinded to the group identity. The modified-limb placing test (MLPT) was used to assess the sensorimotor integration of the forelimb and the hind limb (Song et al., 2003). First, the rat was suspended at 10 cm above a table, and the stretch of the forelimbs toward the table was evaluated as follows: normal stretch, 0 points; abnormal flexion, 1 point. Next the rat was positioned along the edge of the table, and its forelimbs were suspended over the edge of the table and allowed to move freely. Each limb (forelimb, second task; hind limb, third task) was pulled down gently, and retrieval and placement were checked. Finally, the rat was placed toward the table edge to check for lateral placement of the forelimb. These tasks were scored in the following manner: normal performance, 0 point; performance with a delay (2 sec) and/or incomplete, 1 point; no performance, 2 points. Seven points indicate maximal neurological deficit, and 0 point indicates normal performance.

Neurological severity score (NSS) was adopted from previous reports (Chen et al., 2001; Narantuya et al., 2010). NSS is a composite of motor, sensory, reflex, and balance tests (Table 1). One point is awarded for the inability to perform a test or for the lack of a tested reflex. The rat was trained to be familiar with the testing environment before ICH.

Statistical analyses

All numerical values are expressed as mean ± standard deviation. Data were analyzed with student's *t*-test for two-sample assessment or one-way analysis of variance followed by Turkey's test for multiple comparisons. $P < 0.05$ was considered to infer statistical significance.

Table 1. Neurological Severity Scores

		Points
Spontaneous activity	Move around, approach ≧3 walls of the cage	0
	Reach ≧1 upper rim of the cage	1
	Do not rise up at all	2
	Do not move at all	3
Motor tests	Placing rats on the floor	
	Normal walk, straight path	0
	Curvilinear path	1
	Walk only in circles	2
	Fall down to the paretic side	3
	Raising rat by the tail	
	Flexion of forelimb	1
	Flexion of hindlimb	1
	Head moved >10 to vertical axis w/in 30 sec	1
Sensory tests	Placing test (visual test)	1
	Placing test (tactile test)	2
	Proprioceptive test (deep sensation, pushing paw against the table edge to stimulate limb muscles)	3
Beam balance tests	Balances with steady posture	0
	Grasps side of beam	1
	Hugs the beam and one limb falls down from the beam	2
	Hugs the beam and two limbs fall down from the beam, or spins on beam (>60 sec)	3
	Attempts to balance on the beam but falls off (>40 sec)	4
	Attempts to balance on the beam but falls off (>20 sec)	5
	Falls off: no attempt to balance or hang onto the beam (<20 sec)	6
Reflexes absent and abnormal movements	Pinna reflex (head shake when touching the auditory meatus)	1
	Corneal reflex (eye blink when lightly touching the cornea with cotton)	1
	Startle reflex (motor response to a brief noise from snapping a clipboard paper)	1
	Seizures, myoclonus, myodystony	1
Maximal points		25

One point is awarded for inability to perform the tasks or for the lack of a tested reflex.

Results

Experimental RVHT

One rat had severe weight loss after renal artery constriction and was euthanized at 4 weeks after surgery. All other rats had progressive weight gain after renal artery constriction or sham operation and remained alert throughout the experimental period. There was no significant difference in body weight between the sham-operated group and the RVHT group at 5 weeks after operation. Compared with the sham-operated rats, the RVHT rats developed cardiac hypertrophy, but without signs of congestive heart failure, as well as right kidney hypertrophy (Table 2).

Table 2. Body, Heart, and Kidney Weights, and Blood Glucose in RVHT Rats and Sham-Operated Rats 5 Weeks Post-Surgery

	Control	*RVHT*	*RVHT vs control* (p)
Body weight (g)	431.3 ± 42.8	455.8 ± 46.9	0.09
Heart weight (g)	1.3 ± 0.2	1.8 ± 0.2	**<0.001**
Left kidney weight (g)	1.8 ± 0.1	1.7 ± 0.3	0.46
Right kidney weight (g)	1.8 ± 0.1	2.3 ± 0.3	**<0.001**
Blood glucose (mmol/L)	9.1 ± 1.8	8.4 ± 2.9	0.92

Data denote mean ± SD.

Before renal artery constriction, SBP was 114.3 ± 5.2 mmHg. In sham-operated rats, there was no significant change of SBP within 7 weeks after operation. In the RVHT rats, SBP gradually increased after operation with SBP and was >150 mmHg at 4 weeks after surgery. From 6 to 8 weeks after surgery, SBP ranged from 170 mmHg to 190 mmHg in the RVHT rats. At 11 weeks after surgery, PAS staining showed cellular hyperplasia in juxtaglomerular apparatus and renal corpuscle of the left kidney. Fibrinoid necrosis, hyaline degeneration, hyperplasia of the wall of arterioles or small arteries, microaneurysms, and thrombotic vascular occlusions were not observed in the cerebral vasculature at 11 weeks after renal artery constriction (Fig. 1C,D) or sham operation (Fig. 1A,B).

Physiological data for ICH model

All rats survived after the ICH until sacrifice at the specified time points. There was no difference in body weight, blood glucose levels (Table 2), rectal temperature, and respiratory rates (data not shown) between the RVHT and normotensive rats on the day of ICH induction. The body weight was reduced after surgery. The RVHT rats had significant weight loss after ICH: 1 day (−32.8 ± 11.5 g, n = 24), 3 days (−39.3 ± 24.8 g, n = 11), 7 days (−40.2 ± 15.8 g, n = 11), 10 days (−35.5 ± 12.5 g, n = 11), and 14 days (−29.0 ± 11.0 g, n = 6). The normotensive rats also had significant weight loss after ICH: 1 day (−22.9 ± 11.6 g, n = 25), 3 days (−24.6 ± 16.2 g, n = 12), 7 days (−21.2 ± 15.1 g, n = 12) and 10 days (−20.9 ± 17.6 g, n = 12). When compared to the normotensive rats, the RVHT rats had greater weight loss 1 day, 3 days, 7 days, and 10 days after ICH. Weight loss peaked on day 3 in the normotensive rats and day 7 in the RVHT rats. From that time on, rat body weight gradually increased (Fig. 2A).

Acute BP elevation and heart rate

Figure 2B illustrates the temporal changes of MAP between 10 min prior to and 240 min after ICH onset. The RVHT rats had a significantly higher MAP (131.9 ± 12.6 mmHg) than that of the normotensive rats (85.7 ± 11.5 mmHg; Fig. 2B) before ICH induction. MAP was significantly higher in the RVHT rats when compared to normotensive rats during the 240 min period after ICH. In the normotensive rats, MAP increased to 89.5 mmHg at 30 min after ICH and remained elevated at all time points except at 60 min. Similarly in the RVHT rats, MAP was increased to 138.9 mmHg at 30 min after ICH and remained elevated at all time points except at 90 min (Fig. 2B).

There was no significant change in heart rate during the first 240 min after ICH in the RVHT rat. However, there was a significant increase of heart rate in the normotensive rats at

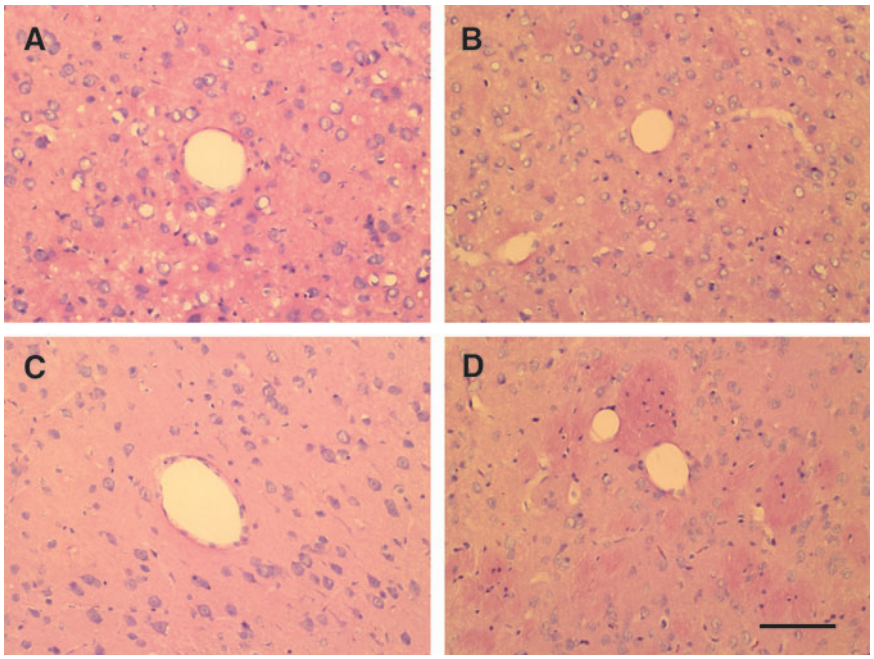

FIG. 1. HE staining of brains 11 weeks after left renal artery constriction. There is no significant morphological change of blood vessels in the RVHT rat (**A**,**B**) compared to the normotensive rats (**C**,**D**). Cerebral cortex (**A**,**B**); striatum (**C**,**D**); HE, hematoxylin and eosin; scale bar, 100 μm. Color image is available online at www.liebertonline.com/neu

120 min, 150 min, and 180 min after ICH (Fig. 2C). There was no significant difference in heart rate between the two groups at all time points.

Hematoma volume and brain swelling

Using spectrophotometric assay of hemoglobin content, hematoma volume was 12.4 ± 3.5 μL in the normotensive rats ($n = 8$) and 20.1 ± 8.1 μL in the RVHT rats ($n = 5$; Fig. 3C) 1 day after ICH. The hematoma volume was increased by 60% in the RVHT rats when compared with the normotensive rats (Fig. 3A–C).

On day 1, the hemorrhagic area represented the lesion area. Lesion volume was 31.8 ± 4.4 μL in the normotensive rats ($n = 5$) and 44.4 ± 10.7 μL in the RVHT rats ($n = 5$). Both groups had significant ipsilateral brain swelling. Moreover, the RVHT rats ($20.1 \pm 8.1\%$, $n = 5$) had greater brain swelling when compared with the normotensive rats ($12.4 \pm 3.5\%$, $n = 5$; Fig. 3D).

Cell proliferation

ICH stimulated progenitor cell proliferation in the ipsilateral hemisphere in both the normotensive (Fig. 4C) and hypertensive rats (Fig. 4D). RVHT rats had a greater increase in the number of proliferating cells (15.0 ± 5.7 cells/mm^2, $n = 5$) in the ipsilateral striatum when compared with the normotensive rats (6.2 ± 1.3 cells/mm^2, $n = 5$; Fig. 4E) 10 days after ICH. Double staining with BrdU and nestin revealed that more than 95% of BrdU positive cells were also positive for nestin (Fig. 4F1–F3,G1–G3).

Apoptosis

TUNEL positive cells were seen within the hematoma as well as in the perihematomal areas 10 days after ICH (Fig. 5A,B). Quantitative analysis revealed a significantly increased number of TUNEL positive cells in the perihematomal area of the RVHT rats compared with the normotensive rats (4.4 ± 0.6 cells/mm^2 versus 1.5 ± 0.5 cells / mm^2, $n = 3$ in each group; Fig. 5C).

Lesion volume on day 21

On day 21, the lesion contained cell debris and fluid-filled spaces (Fig. 6A). There was a clear line of demarcation between the lesion area and surrounding brain parenchyma. The lesion volume was significantly decreased compared to that on day 1 after ICH in both groups. However, the hypertensive rats had a greater lesion volume 21 days after ICH (14.8 ± 2.7 μL versus 5.9 ± 3.1 μL; Fig. 6B). Moreover, both groups had obvious brain tissue loss and lateral ventricle enlargement, which were more severe in the RVHT group. Volume of lost brain tissue was 34.8 ± 4.7 μL in the RVHT rats ($n = 6$) and 24.8 ± 2.2 μL in the normotensive rats ($n = 7$). Volume of lateral ventricle was 20.1 ± 8.0 μL in the RVHT rats ($n = 6$) and 7.0 ± 3.1 μL in the normotensive rats ($n = 8$, Fig. 6B). Three weeks following sham ICH, there was no significant difference in lateral ventricle volume between the normotensive and hypertensive rats (4.1 ± 0.4 μL, $n = 4$ versus 4.2 ± 0.5 μL, $n = 4$). However, both the normotensive and hypertensive animals revealed significantly enlarged lateral ventricle 21 days after ICH when compared to sham ICH animals.

Functional deficits

No rats had spontaneous stroke within 11 weeks after renal artery constriction. The RVHT rats had more profound sensorimotor deficits than the normotensive rats 1 day after ICH as assessed by MLPT at all time points (Fig. 7A). In addition, the RVHT rats had a higher NSS score than that of normotensive rats at all time points (Fig. 7B).

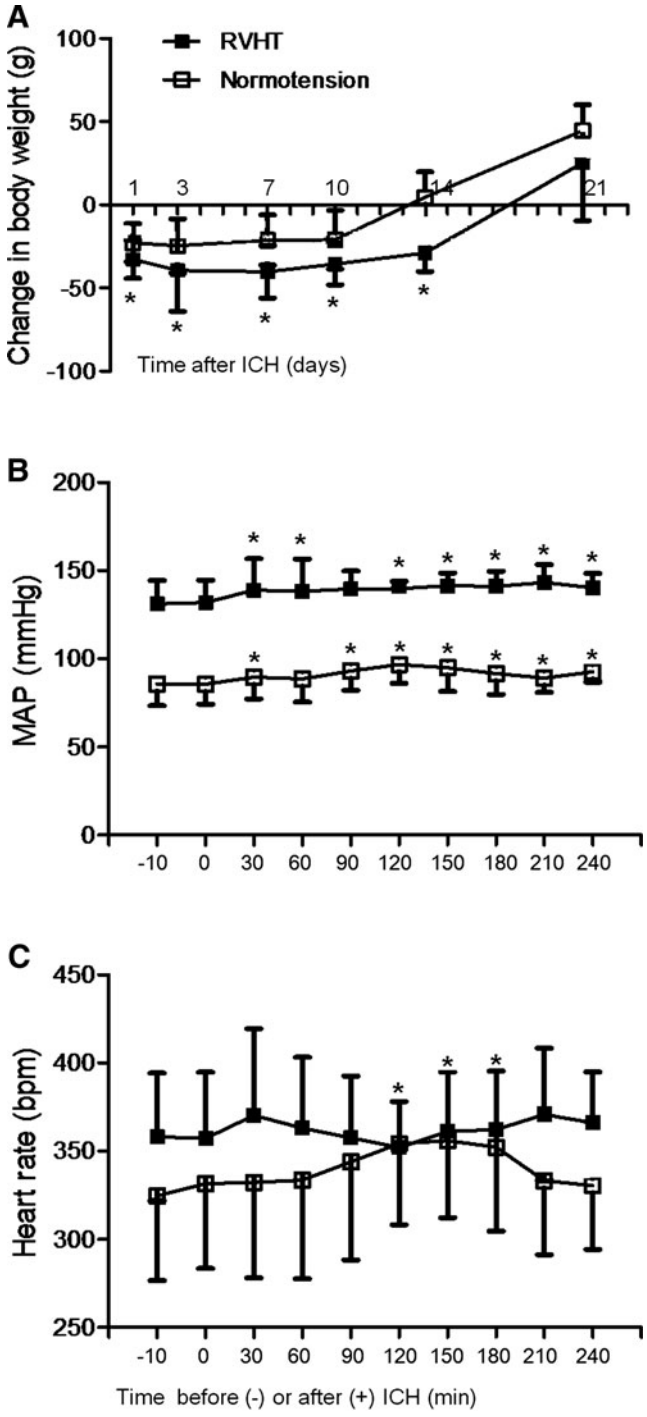

FIG. 2. Changes in body weight, mean artery pressure (MAP), and heart rate after ICH. The RVHT rats have severer weight loss 1, 3, 7, and 10 days after ICH compared to the normotensive rats (**A**; $*p < 0.05$ versus the normotensive group). Temporal changes in MAP (**B**) and heart rate (**C**) in the normotensive ($n = 6$ per time point) and RVHT ($n = 5$ per time point) rats are depicted between 10 min before and 240 min after ICH ($*p < 0.05$ compared to 0 min). Following induction of ICH, both the normotensive and RVHT rats have acute BP elevation. The normotensive rats have a significant increase of heart rate from 120 to 180 min after ICH while the RVHT rats do not show any significant changes during the period.

Discussion

In the present study, we investigated how elevated BP would affect physiological parameters, brain histology, and neurological function in a rat ICH model. Following ICH, elevated BP increased acute and sub-acute brain injury as measured by hematoma volume, brain swelling and apoptosis, aggravated brain degeneration as measured by brain tissue loss and lateral ventricle enlargement, and worsened functional deficits. On the other hand, more endogenous NSCs were present in the ipsilateral striatum in the hypertensive rats.

Successful bench-to-bedside translation of an effective stroke therapy demands experimental research conducted in comparable conditions relevant to patients (Endres et al., 2008). Hypertension, which occurs in nearly 30% of the world's population and 60–70% of ICH patients (Thrift et al., 1998; Tikhonoff et al., 2009), affects not only the pathophysiology of ICH, but also the potential effects of treatment. An ideal experimental ICH model should include hypertension. In this study, we used a well-established non-genetic 2K1C hypertension model to evaluate the effects of elevated BP on ICH-related injury.

Severe long-term hypertension may cause spontaneous stroke, manifesting as small hemorrhagic and infarct transparent lesions in the brain (Shaver et al., 1992; Zeng, et al., 1998). The rats with spontaneous ICH have the corresponding sensorimotor dysfunction. In our study, BP of the RVHT rats gradually increased and stabilized around 160–190 mmHg. We examined the brain histology at 11 weeks after renal artery constriction. During this period, no rat showed features of spontaneous stroke, and brain sections were unremarkable. The 2K1C model of RVHT is a high renin form of hypertension. In this model, end-organ damage includes cardiac hypertrophy (defined as a 20–50% increase in cardiac size) and hypertrophy of the contralateral kidney (Pinto et al., 1998). In the present study, the RVHT rats had hypertrophy of the heart and contralateral kidney at 5 weeks after renal artery constriction. However, features of cardiac failure were not seen in the RVHT rats during the study.

Acute BP elevation is common in ICH patients (Qureshi, 2008). It may be attributed to the direct damage of brain tissue regulating cardiovascular function and other factors, which impair parasympathetic activity and baroreceptor sensitivity, such as stress responses, headache, and urinary retention (Qureshi, 2008). In this study, both the normotensive and hypertensive rats had acute BP elevation after ICH onset. BP measurement via femoral artery was obtained under anesthesia. Anesthetics can affect cardiovascular, biochemical, and hormonal responses following injury in animals and humans (Hempenstall et al., 1986; Nout et al., 2011). The effects of anesthetics and stress response on MAP after ICH could not be excluded. Anesthesia-related BP change after ICH should be investigated in the future. Importantly, the optimal management of acute BP elevation in ICH patients remains controversial (Qureshi et al., 2010; Tikhonoff, et al., 2009), so this ICH model in hypertensive rats can be useful. Moreover, the normotensive rats showed increased heart rate during the hyperacute phase, which may reflect the cardiovascular regulation following ICH. Nevertheless, increased heart rate was not seen in the hypertensive animal, and this may be due to an altered cardiovascular response in RVHT. Additional studies

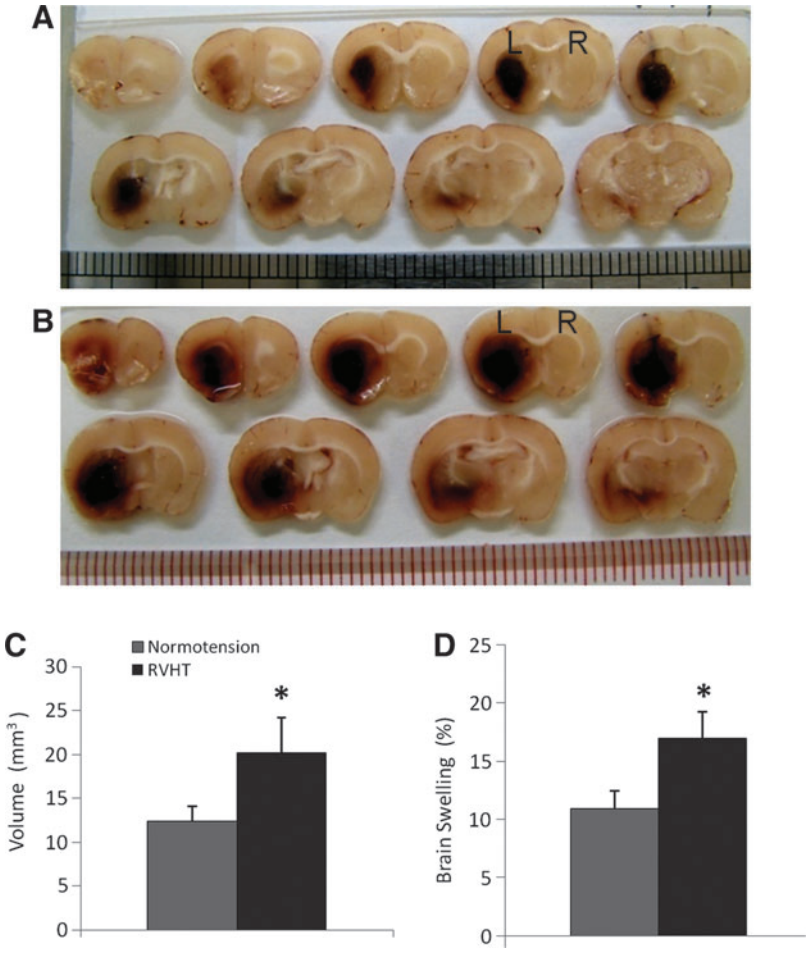

FIG. 3. Brain hemorrhagic lesion and brain swelling 24 h after ICH. Series of coronal brain images from a normal rat (**A**) and a RVHT rat (**B**) illustrate the location of the hemorrhagic lesion. L, left hemisphere; R, right hemisphere. The RVHT rats ($n=8$) demonstrate a larger hematoma volume compared to the normotensive rats ($n=5$, **C**). The RVHT rats ($n=5$) have greater brain swelling compared to the normotensive rats ($n=5$). *$p<0.05$ versus normotensive group. Color image is available online at www.liebertonline.com/neu

on the changes of neural-hormone system as well as heart histology and function would be helpful in revealing the underlying mechanisms. The temperature profiles and blood glucose levels in both groups were similar and within the normal range. Thus, hypothermia, which reduces cell death after ischemia (Colbourne et al., 1997; Dietrich et al., 1996) and brain edema after ICH (Fingas et al., 2009; Kawanishi et al., 2008), as well as hyperglycemia, which increases cell death after ICH (Song et al., 2003), were not found to be contributing factors in this study.

Many clinical studies have show that hematoma growth is common within the first 24 h after symptom onset; such growth is associated with increased mortality and poor functional outcomes (Davis et al., 2006; Kazui et al., 1996). Further clinical studies have demonstrated a significant association between high SBP and hematoma growth (Fujii et al., 1998; Ohwaki et al., 2004; Willmot et al., 2004). However, there is little experimental data on the hematoma volume in animals with elevated BP. In our study, high BP significantly increased hematoma volume in the brain at 24 h after collagenase injection in the RVHT rats. A plausible explanation is the hyperactive hemodynamics of hypertensive condition. The 2K1C model of RVHT demonstrates increased activities of both systemic and tissue RAS in the heart, aorta, lung, and kidney (Morishita et al., 1991, 1993). RAS plays an important role in hemodynamic regulation. Ang II, a potent vasoconstrictor, increases BP and cerebral blood flow (Mogielnicki et al., 2005), which may impede the hemostasis. It is also possible that the disturbances in cerebral autoregulation in hypertensive condition or subsequent to ICH in the RVHT rats may play a role. Assessment of the haemodynamics in this hypertensive ICH model by PET or fMRI techniques may reveal the exact mechanisms. Recently it has been shown that Ang II enhances prothrombotic activity and promotes *in vivo* thrombosis (Kaminska et al., 2005; Mogielnicki, et al., 2005). We observed increased bleeding and brain injury in the RVHT rats. Therefore, activated RAS in the RVHT rats leads to aggravated hemorrhage and brain injury. Whether the plasma coagulation and fibrinolytic parameters in the RVHT rats are compromised needs to be addressed in future studies. Another explanation for the differences in hematoma volume is compromised cerebrovasculature in the hypertensive rats. Although HE staining did not show significant damages of the cerebral blood vessels, there may be significant changes at sub-microscopic level to account for the aggravated brain injury in the RVHT rats.

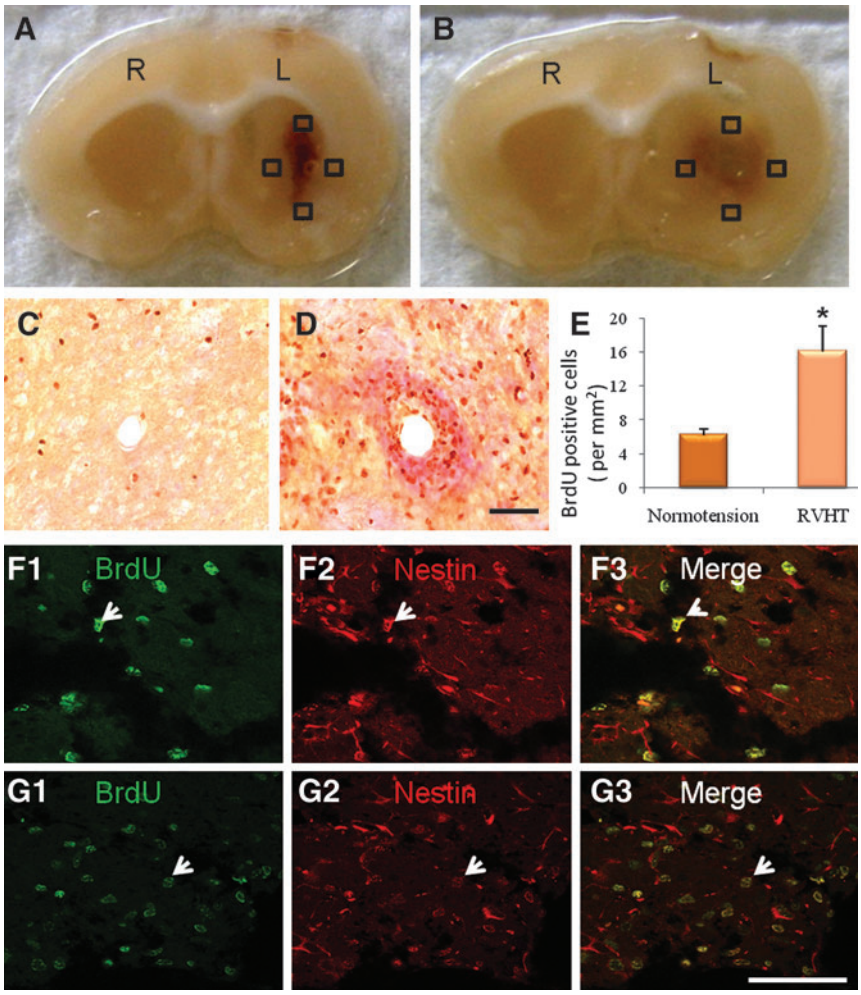

FIG. 4. Cell proliferation in the perihematomal areas 10 days after ICH. Typical hemorrhagic lesion is shown in a normotensive rats (**A**) and a RVHT rat (**B**). L, left hemisphere; R, right hemisphere. Cells double-labeled with BrdU and nestin are counted in four randomly selected grids (black boxes show examples) at the edge of the hematoma (**A**,**B**). Representative microscope images show proliferating cells on the edge of the hemorrhagic lesion in a normotensive rat (**C**) and a RVHT rat (**D**). Scale bar, 100 μm (**C**,**D**). Quantitative analysis of BrdU positive cells on the edge of hematoma using an unbiased stereological manner reveals that the RVHT rats have a greater density of proliferating cells than the normotensive rats (**E**). $^*p < 0.01$ versus normotensive group. Double-staining with BrdU and nestin in the perihematomal areas reveals that the majority of BrdU positive cells are also nestin positive. Note double-labeling (white arrows) for BrdU and nestin in a normotensive rat (**F1–F3**) and a hypertensive rat (**G1–G3**). Scale bar, 70 μm in **F1–F3** and **G1–G3**. Color image is available online at www.liebertonline.com/neu

Although ICH patients have a mortality rate of 31% 7 days after onset (Flaherty et al., 2006; Fogelholm et al., 2005), mortality rate was zero within 21 days after ICH in both the normotensive and hypertensive rats. The mean lesion volume in the RVHT rats was 44.4 μL, and the hemorrhagic lesion was located in the left basal ganglia, without extending to the cortex or lateral ventricle. In contrast, the autologous blood injection ICH model with a hematoma volume of 75 μL has a mortality rate around 50% (Marinkovic et al., 2009). It would be interesting to evaluate the effect of elevated BP on the mortality rate using a higher dose of collagenase IV to induce a larger hemorrhagic lesion.

In the present study, severe sensorimotor deficits were seen in both the normotensive and hypertensive rats, allowing us to evaluate treatments for functional recovery. Mechanisms of ICH-related brain injury include the mass effect, inflammation, apoptosis, and toxic effects of blood degradation products (Chu et al., 2004b; Jung et al., 2004; Lee et al., 2006; Wang et al., 2002). The rats with elevated BP had worse brain tissue loss, weight loss, and functional deficits after ICH. The mechanisms accounting for the greater injury in the RVHT rats are not clearly known. Increased hematoma volume in the RVHT rats 1 day after ICH suggests aggravated primary brain injury. A series of reactive responses, such as brain swelling, inflammation, and apoptosis may lead to secondary brain damage. Meanwhile, RVHT also activates systemic and tissue RAS. Previous reports have shown that inhibition of RAS in the brain reduces infarct volume, attenuates inflammation and oxidative stress, and modulates the nitric-oxide synthase isoenzymes in animal stroke models, as well as improves functional outcome in stroke patients (Ando et al., 2004a,b; Dai et al., 1999; Ito et al., 2002; Jung et al., 2007; Mark and Davis, 2000; Nishimura et al., 2000; Werner et al., 1991; Yabuuchi et al., 1999; Zhou et al., 2005). Therefore, the increased

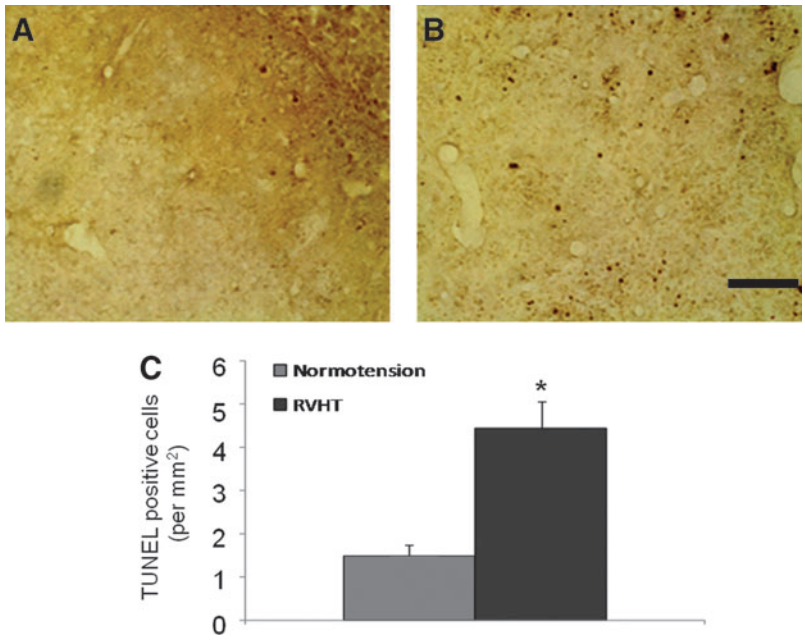

FIG. 5. TUNEL staining 10 days after ICH. Representative images illustrate apoptosis in the ipsilateral striatum in a normotensive rat (**A**) and a RVHT rat (**B**). Quantitative analysis reveals that the number of TUNEL positive cells is increased in the RVHT rats (**C**). $n=3$ per group, $^{*}p<0.05$ versus normotensive group. Color image is available online at www.liebertonline.com/neu

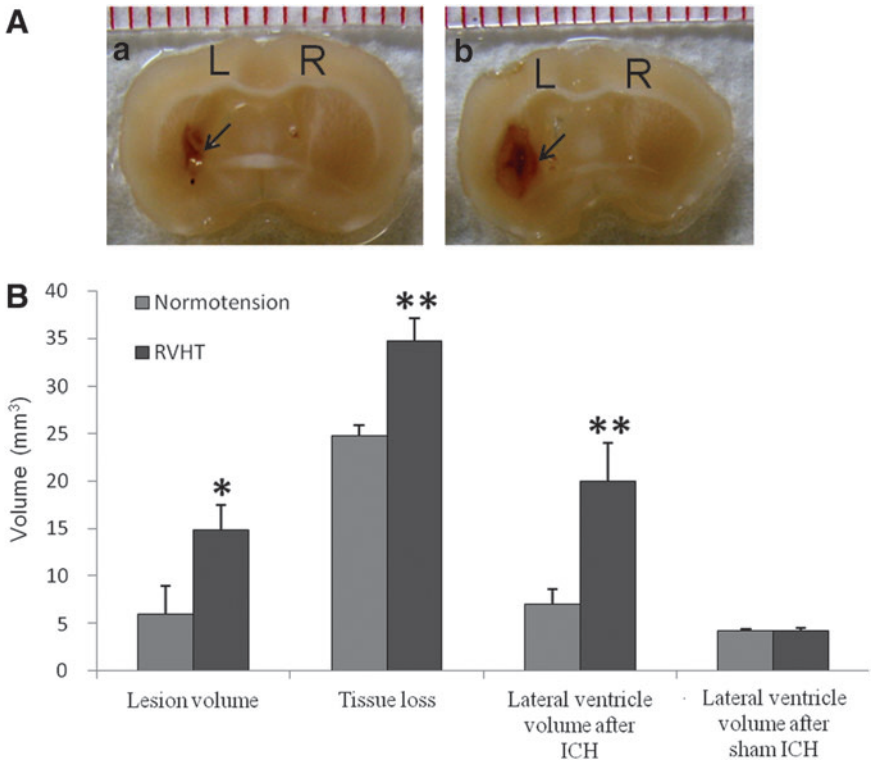

FIG. 6. Lesion volume, brain tissue loss, and lateral ventricle enlargement 21 days after ICH. The representative brain coronal sections (**A**) show the lesion area of comparable sites from a normal rat (**a**) and a RVHT rat (**b**). L, left hemisphere; R, right hemisphere. Black arrows denote the edge of the lesion. Upon quantification (**B**), the RVHT rats ($n=6$) have a larger lesion volume, greater tissue loss, and a larger lateral ventricle compared to the normotensive rats ($n=7$). $^{*}p<0.05$, $^{**}p<0.01$ versus normotensive group. Color image is available online at www.liebertonline.com/neu

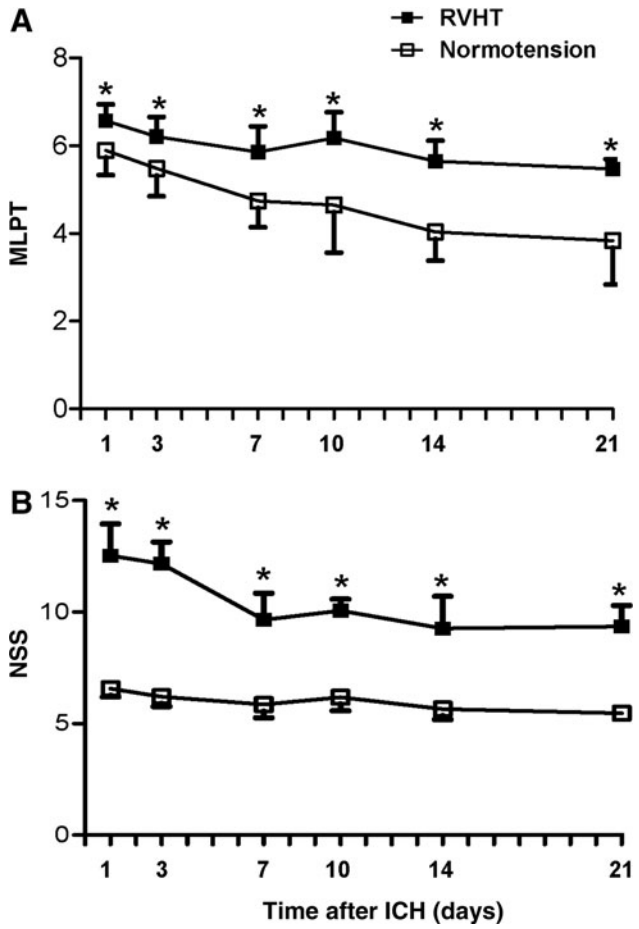

FIG. 7. MLPT and NSS assessed on days 1, 3, 7, 10, 14, and 21 after ICH. The RVHT rats have more severe sensorimotor functional deficits at all time points compared to the normotensive rats as assessed by MLPT (**A**). The RVHT rats also have severe functional deficits at all time points compared to the normotensive rats as assessed by NSS (**B**). $n = 6$ to 11 rats per time point in each group. $p < 0.05$ compared to normotensive group.

brain injury in the RVHT rats may be mediated via the activated RAS. Further studies on the effect of RAS inhibition on ICH-related brain injury in the RVHT rats will be useful to elucidate this hypothesis.

Increased endogenous NSC proliferation in the ipsilateral hemisphere following ICH has been previously seen in both humans and animals (Shen et al., 2008; Tang et al., 2004). We observed that elevated BP further enhanced endogenous NSC recruitment in the ipsilateral striatum. The mechanisms of enhanced NSC recruitment in the ipsilateral striatum are not clear. Several studies have shown that inflammatory stimuli recruit NSCs to the hematoma site (Imitola et al., 2004; Wang et al., 2007). Elevated BP may increase the inflammatory stimuli, and further study is warranted to identify the mechanisms. Unfortunately, this self-repair manoeuvre of injured brain did not translate into improved functional recovery 21 days after ICH. It may be that a longer time, such as 6–8 weeks, is needed for the NSCs to differentiate and incorporate into the brain circuits to compensate for the lost brain functions.

In summary, elevated BP in our RVHT model did not cause spontaneous stroke within the study period. Elevated BP led to worse acute and sub-acute brain injury as well as brain degeneration in a rat ICH model. Despite enhanced NSC recruitment in the perihematomal areas, the hypertensive rats had substantial and persistent neurological deficits. Thus, the ICH model in rats with elevated BP closely mimics human ICH-related pathophysiology, brain histology, and functional deficits, provides a platform to study the mechanisms of ICH-induced brain injury, and can be used to evaluate potential therapies for ICH patients.

Acknowledgments

This work was supported by a General Research Fund of Research Grants Council (HKU763109M) and Committee on Research and Conference Grants (200707176018, 200807176052, 201007176091).

Author Disclosure Statement

There are no financial interests to disclose.

References

Al-Sarraf, H., and Philip, L. (2003). Effect of hypertension on the integrity of blood brain and blood CSF barriers, cerebral blood flow and CSF secretion in the rat. Brain Res. 975(1-2), 179–188.

Ando, H., Jezova, M., Zhou, J., and Saavedra, J.M. (2004a). Angiotensin II AT1 receptor blockade decreases brain artery inflammation in a stress-prone rat strain. Ann. NY Acad. Sci. 1018, 345–350.

Ando, H., Zhou, J., Macova, M., Imboden, H., and Saavedra, J. M. (2004b). Angiotensin II AT1 receptor blockade reverses pathological hypertrophy and inflammation in brain microvessels of spontaneously hypertensive rats. Stroke 35(7), 1726–1731.

Auriat, A., Plahta, W.C., McGie, S.C., Yan, R., and Colbourne, F. (2005). 17 beta-estradiol pretreatment reduces bleeding and brain injury after intracerebral hemorrhagic stroke in male rats. J. Cereb. Blood Flow Metab. 25(2), 247–256.

Broderick, J., Connolly, S., Feldmann, E., Hanley, D., Kase, C., Krieger, D., Mayberg, M., Morgenstern, L., Ogilvy, C.S., Vespa, P., and Zuccarello, M. (2007). Guidelines for the management of spontaneous intracerebral hemorrhage in adults: 2007 update: a guideline from the American Heart Association/ American Stroke Association Stroke Council, High Blood Pressure Research Council, and the Quality of Care and Outcomes in Research Interdisciplinary Working Group. Stroke 38(6), 2001–2023.

Brott, T., Thalinger, K., and Hertzberg, V. (1986). Hypertension as a risk factor for spontaneous intracerebral hemorrhage. Stroke, 17(6), 1078–1083.

Brunner, H.R., Kirshman, J.D., Sealey, J.E., and Laragh, J.H. (1971). Hypertension of renal origin: evidence for two different mechanisms. Science 174(16), 1344–1346.

Caplan, L.R. (1992). Intracerebral haemorrhage. Lancet, 339(8794), 656–658.

Chen, J., Li, Y., Wang, L., Zhang, Z., Lu, D., Lu, M., and Chopp, M. (2001). Therapeutic benefit of intravenous administration of bone marrow stromal cells after cerebral ischemia in rats. Stroke 32(4), 1005–1011.

Choudhri, T.F., Hoh, B.L., Solomon, R.A., Connolly, E.S., Jr., and Pinsky, D.J. (1997). Use of a spectrophotometric hemoglobin assay to objectively quantify intracerebral hemorrhage in mice. Stroke 28(11), 2296–2302.

Chu, K., Jeong, S.W., Jung, K. H., Han, S.Y., Lee, S.T., Kim, M., and Roh, J.K. (2004a). Celecoxib induces functional recovery after intracerebral hemorrhage with reduction of brain edema and perihematomal cell death. J. Cereb. Blood Flow Metab. 24(8), 926–933.

Chu, K., Jung, K.H., Jeong, S.W., Kim, M., and Roh, J.K. (2004b). Celecoxib induces functional recovery after intracerebral hemorrhage with reduction of brain edema and perihematomal cell death. Stroke 35(1), 330–330.

Colbourne, F., Sutherland, G., and Corbett, D. (1997). Post-ischemic hypothermia—critical appraisal with implications for clinical treatment. Mol. Neurobiol. 14(3), 171–201.

Dai, W.J., Funk, A., Herdegen, T., Unger, T., and Culman, J. (1999). Blockade of central angiotensin AT(1) receptors improves neurological outcome and reduces expression of AP-1 transcription factors after focal brain ischemia in rats. Stroke 30(11), 2391–2398; discussion 2398–2399.

Davis, S.M., Broderick, J., Hennerici, M., Brun, N.C., Diringer, M.N., Mayer, S.A., Begtrup, K., and Steiner, T. (2006). Hematoma growth is a determinant of mortality and poor outcome after intracerebral hemorrhage. Neurology 66(8), 1175–1181.

DeForrest, J.M., Knappenberger, R.C., Antonaccio, M.J., Ferrone, R.A., and Creekmore, J.S. (1982). Angiotensin II is a necessary component for the development of hypertension in the two kidney, one clip rat. Am. J. Cardiol. 49(6), 1515–1517.

Dietrich, W.D., Busto, R., Globus, M.Y.T., and Ginsberg, M.D. (1996). Brain damage and temperature: cellular and molecular mechanisms. Cell. Mol. Mechan. Ischem. Brain Dam. 71, 177–197.

Endres, M., Engelhardt, B., Koistinaho, J., Lindvall, O., Meairs, S., Mohr, J.P., Planas, A., Rothwell, N., Schwaninger, M., Schwab, M.E., Vivien, D., Wieloch, T., and Dirnagl, U. (2008). Improving outcome after stroke: overcoming the translational roadblock. Cerebrovasc. Dis 25(3), 268–278.

Fingas, M., Penner, M., Silasi, G., and Colbourne, F. (2009). Treatment of intracerebral hemorrhage in rats with 12 h, 3 days and 6 days of selective brain hypothermia. Exp. Neurol. 219(1), 156–162.

Flaherty, M.L., Haverbusch, M., Sekar, P., Kissela, B., Kleindorfer, D., Moomaw, C.J., Sauerbeck, L., Schneider, A., Broderick, J.P., and Woo, D. (2006). Long-term mortality after intracerebral hemorrhage. Neurology 66(8), 1182–1186.

Fogelholm, R., Murros, K., Rissanen, A., and Avikainen, S. (2005). Long term survival after primary intracerebral haemorrhage: a retrospective population based study. J. Neurol. Neurosurg. Psychiatry 76(11), 1534–1538.

Fujii, Y., Takeuchi, S., Sasaki, O., Minakawa, T., and Tanaka, R. (1998). Multivariate analysis of predictors of hematoma enlargement in spontaneous intracerebral hemorrhage. Stroke 29(6), 1160–1166.

Gebel, J.M., and Broderick, J.P. (2000). Intracerebral hemorrhage. Neurol. Clin. 18(2), 419–438.

Gonzalez-Darder, J.M., and Duran-Cabral, J. (1990). Experimental intracerebral haemorrhage in normotensive and spontaneously hypertensive rats. Acta Neurochir. (Wien) 107(3-4), 102–107.

Hempenstall, P.D., Campbell, J.P., Bajurnow, A.T., Reade, P.C., McGrath, B., and Harrison, L.C. (1986). Cardiovascular, biochemical, and hormonal responses to intravenous sedation with local analgesia versus general anesthesia in patients undergoing oral surgery. J. Oral Maxillofac. Surg. 44(6), 441–446.

Imitola, J., Raddassi, K., Park, K.I., Mueller, F.J., Nieto, M., Teng, Y.D., Frenkel, D., Li, J., Sidman, R.L., Walsh, C.A., Snyder, E.Y., and Khoury, S.J. (2004). Directed migration of neural stem cells to sites of CNS injury by the stromal cell-derived factor 1alpha/CXC chemokine receptor 4 pathway. Proc. Natl. Acad. Sci. USA 101(52), 18117–18122.

Ito, T., Yamakawa, H., Bregonzio, C., Terron, J.A., Falcon-Neri, A., and Saavedra, J.M. (2002). Protection against ischemia and improvement of cerebral blood flow in genetically hypertensive rats by chronic pretreatment with an angiotensin II AT1 antagonist. Stroke 33(9), 2297–2303.

Jung, K.H., Chu, K., Jeong, S.W., Han, S.Y., Lee, S.T., Kim, J.Y., Kim, M., and Roh, J.K. (2004). HMG-CoA reductase inhibitor, atorvastatin, promotes sensorimotor recovery, suppressing acute inflammatory reaction after experimental intracerebral hemorrhage. Stroke 35(7), 1744–1749.

Jung, K.H., Chu, K., Lee, S.T., Kim, S.J., Song, E.C., Kim, E.H., Park, D.K., Sinn, D. I., Kim, J.M., Kim, M., and Roh, J.K. (2007). Blockade of AT1 receptor reduces apoptosis, inflammation, and oxidative stress in normotensive rats with intracerebral Hemorrhage. J Pharmacol Exp. Ther. 322(3), 1051–1058.

Kaminska, M., Mogielnicki, A., Stankiewicz, A., Kramkowski, K., Domaniewski, T., Buczko, W., and Chabielska, E. (2005). Angiotensin II via AT1 receptor accelerates arterial thrombosis in renovascular hypertensive rats. J. Physiol. Pharmacol. 56(4), 571–585.

Kawanishi, M., Kawai, N., Nakamura, T., Luo, C., Tamiya, T., and Nagao, S. (2008). Effect of delayed mild brain hypothermia on edema formation after intracerebral hemorrhage in rats. J. Stroke Cerebrovasc. Dis. 17(4), 187–195.

Kazui, S., Naritomi, H., Yamamoto, H., Sawada, T., and Yamaguchi, T. (1996). Enlargement of spontaneous intracerebral hemorrhage. Incidence and time course. Stroke 27(10), 1783–1787.

Koletsky, S., Pavlicko, K.M., and Rivera-Velez, J.M. (1971). Renin-angiotensin activity in hypertensive rats with a single ischemic kidney. Lab. Invest. 24(1), 41–44.

Kurtz, T.W., Griffin, K.A., Bidani, A.K., Davisson, R.L., and Hall, J.E. (2005). Recommendations for blood pressure measurement in animals—summary of an AHA Scientific Statement from the Council on High Blood Pressure Research, Professional and Public Education Subcommittee. Arterioscler. Thromb. Vasc. Biol. 25(3), 478–479.

Lee, S.T., Chu, K., Sinn, D.I., Jung, K.H., Kim, E.H., Kim, S.J., Kim, J.M., Ko, S.Y., Kim, M., and Roh, J.K. (2006). Erythropoietin reduces perihematomal inflammation and cell death with eNOS and STAT3 activations in experimental intracerebral hemorrhage. J. Neurochem. 96(6), 1728–1739.

Leenen, F.H., and de Jong, W. (1971). A solid silver clip for induction of predictable levels of renal hypertension in the rat. J. Appl. Physiol. 31(1), 142–144.

Lerman, L.O., Chade, A.R., Sica, V., and Napoli, C. (2005). Animal models of hypertension: an overview. J. Lab. Clin. Med. 146(3), 160–173.

MacLellan, C.L., Girgis, J., and Colbourne, F. (2004). Delayed onset of prolonged hypothermia improves outcome after intracerebral hemorrhage in rats. J. Cereb. Blood Flow Metab. 24(4), 432–440.

Marinkovic, I., Strbian, D., Pedrono, E., Vekovischeva, O.Y., Shekhar, S., Durukan, A., Korpi, E.R., Abo-Ramadan, U., and Tatlisumak, T. (2009). Decompressive craniectomy for intracerebral hemorrhage. Neurosurgery 65(4), 780–786; discussion 786.

Mark, K.S., and Davis, T.P. (2000). Stroke: development, prevention and treatment with peptidase inhibitors. Peptides 21(12), 1965–1973.

Matsushita, K., Meng, W., Wang, X., Asahi, M., Asahi, K., Moskowitz, M.A., and Lo, E.H. (2000). Evidence for apoptosis after intracerebral hemorrhage in rat striatum. J. Cereb. Blood Flow Metab. 20(2), 396–404.

Mogielnicki, A., Chabielska, E., Pawlak, R., Szemraj, J., and Buczko, W. (2005). Angiotensin II enhances thrombosis

development in renovascular hypertensive rats. Thromb. Haemost. 93(6), 1069–1076.

Morishita, R., Higaki, J., Okunishi, H., Kawamoto, T., Ishii, K., Nakamura, F., Katahira, K., Nagano, M., Mikami, H., Miyazaki, M., et al. (1991). Effect of long-term treatment with an angiotensin-converting enzyme inhibitor on the renin-angiotensin system in spontaneously hypertensive rats. Clin. Exp. Pharmacol. Physiol. 18(10), 685–690.

Morishita, R., Higaki, J., Okunishi, H., Nakamura, F., Nagano, M., Mikami, H., Ishii, K., Miyazaki, M., and Ogihara, T. (1993). Role of tissue renin angiotensin system in two-kidney, one-clip hypertensive rats (Part 2). Am. J. Physiol. 264(3), F510–514.

Narantuya, D., Nagai, A., Sheikh, A. M., Masuda, J., Kobayashi, S., Yamaguchi, S., and Kim, S.U. (2010). Human microglia transplanted in rat focal ischemia brain induce neuroprotection and behavioral improvement. PLoS One 5(7), e11746.

Nishimura, Y., Ito, T., and Saavedra, J.M. (2000). Angiotensin II AT(1) blockade normalizes cerebrovascular autoregulation and reduces cerebral ischemia in spontaneously hypertensive rats. Stroke 31(10), 2478–2486.

Nout, Y.S., Beattie, M.S., and Bresnahan, J. (2011). Severity of locomotor and cardiovascular derangements after experimental high-thoracic spinal cord injury is anesthesia dependent in rats. J Neurotrauma [Epub ahead of print].

Ohwaki, K., Yano, E., Nagashima, H., Hirata, M., Nakagomi, T., and Tamura, A. (2004). Blood pressure management in acute intracerebral hemorrhage: relationship between elevated blood pressure and hematoma enlargement. Stroke 35(6), 1364–1367.

Okamoto, K., Yamamoto, K., Morita, N., Ohta, Y., Chikugo, T., Higashizawa, T., and Suzuki, T. (1986). Establishment and use of the M-strain of stroke-prone spontaneously hypertensive rat. J. Hypertens. 4, S21–S24.

Park, H.K., Chu, K., Lee, S.T., Jung, K.H., Kim, E.H., Lee, K.B., Song, Y.M., Jeong, S.W., Kim, M., and Roh, J.K. (2005). Granulocyte colony-stimulating factor induces sensorimotor recovery in intracerebral hemorrhage. Brain Res. 1041(2), 125–131.

Pinto, Y.M., Paul, M., and Ganten, D. (1998). Lessons from rat models of hypertension: from Goldblatt to genetic engineering. Cardiovasc. Res. 39(1), 77–88.

Qureshi, A.I. (2008). Acute hypertensive response in patients with stroke—pathophysiology and management. Circulation 118(2), 176–187.

Qureshi, A.I., Ezzeddine, M.A., Nasar, A., Suri, M.F., Kirmani, J.F., Hussein, H.M., Divani, A.A., and Reddi, A.S. (2007). Prevalence of elevated blood pressure in 563,704 adult patients with stroke presenting to the ED in the United States. Am. J. Emer. Med. 25(1), 32–38.

Qureshi, A.I., Tariq, N., Divani, A.A., Novitzke, J., Hussein, H.H., Palesch, Y.Y., Martin, R., Dillon, C., Kirmani, J.F., Ezzeddine, M.A., Mohammad, I., Suri, M.F.K., Harris-Lane, P., Suarez, J.I., Feen, E., Selman, W., Murphy, C., Mayer, S.A., Parra, A., Lee, K., Ostapkovich, N., Papamitsakis, N.I.H., Panezai, S., Anyanwu, C., Terry, J., Dickerson, K., Goldstein, J., Wendell, L., Mohammad, Y.M., Jradi, H., Cruz-Flores, S., Holzemer, E., Sung, G., Thomson, V., Ehtisham, A., Brown, B., and C.A.T.A. (2010). Antihypertensive treatment of acute cerebral hemorrhage. Crit. Care Med. 38(2), 637–648.

Shaver, S.W., Wall, K.M., Wainman, D.S., and Gross, P.M. (1992). Regional quantitative permeability of blood-brain barrier lesions in rats with chronic renal hypertension. Brain Res. 579(1), 99–106.

Shen, J., Xie, L., Mao, X., Zhou, Y., Zhan, R., Greenberg, D.A., and Jin, K. (2008). Neurogenesis after primary intracerebral hemorrhage in adult human brain. J Cereb. Blood Flow Metab. 28(8), 1460–1468.

Song, E.C., Chu, K., Jeong, S.W., Jung, K.H., Kim, S.H., Kim, M., and Yoon, B.W. (2003). Hyperglycemia exacerbates brain edema and perihematomal cell death after intracerebral hemorrhage. Stroke 34(9), 2215–2220.

Tang, T., Li, X. Q., Wu, H., Luo, J.K., Zhang, H.X., and Luo, T.L. (2004). Activation of endogenous neural stem cells in experimental intracerebral hemorrhagic rat brains. Chin. Med. J. (Engl) 117(9), 1342–1347.

Thrift, A.G., McNeil, J.J., Forbes, A., Donnan, G.A., and M.R.F.S. (1998). Three important subgroups of hypertensive persons at greater risk of intracerebral hemorrhage. Hypertension 31(6), 1223–1229.

Tikhonoff, V., Zhang, H.F., Richart, T., and Staessen, J.A. (2009). Blood pressure as a prognostic factor after acute stroke. Lancet Neurol. 8(10), 938–948.

Vemmos, K.N., Tsivgoulis, G., Spengos, K., Zakopoulos, N., Synetos, A., Manios, E., Konstantopoulou, P., and Mavrikakis, M. (2004). U-shaped relationship between mortality and admission blood pressure in patients with acute stroke. J. Intern. Med. 255(2), 257–265.

Wakisaka, Y., Miller, J.D., Chu, Y., Baumbach, G.L., Wilson, S., Faraci, F.M., Sigmund, C.D., and Heistad, D.D. (2008). Oxidative stress through activation of NAD(P)H oxidase in hypertensive mice with spontaneous intracranial hemorrhage. J. Cereb. Blood Flow Metab. 28(6), 1175–1185.

Wang, X.Y., Mori, T., Sumii, T., and Lo, E.H. (2002). Hemoglobin-induced cytotoxicity in rat cerebral cortical neurons—caspase activation and oxidative stress. Stroke 33(7), 1882–1888.

Wang, Y., Jin, K., Mao, X. O., Xie, L., Banwait, S., Marti, H.H., and Greenberg, D.A. (2007). VEGF-overexpressing transgenic mice show enhanced post-ischemic neurogenesis and neuromigration. J. Neurosci. Res. 85(4), 740–747.

Werner, C., Hoffman, W.E., Kochs, E., Rabito, S.F., and Miletich, D.J. (1991). Captopril improves neurologic outcome from incomplete cerebral ischemia in rats. Stroke 22(7), 910–914.

Willmot, M., Leonardi-Bee, J., and Bath, P.M. (2004). High blood pressure in acute stroke and subsequent outcome: a systematic review. Hypertension 43(1), 18–24.

Wilson, C., and Byrom, F.B. (1939). Renal changes in malignant hypertension. Lancet 1, 136–139.

Yabuuchi, F., Takahashi, M., Aritake, K., Fujimoto, M., Ito, H., Tsuzaki, M., Akai, T., Yamaguchi, M., Hayashi, S., Nishino, Y., and Brautigam, M. (1999). Post-stroke treatment with imidapril reduces learning deficits with less formation of brain oedema in a stroke-prone substrain of spontaneously hypertensive rats. Fund. Clin. Pharmacol. 13(4), 475–483.

Zeng, J., Zhang, Y., Mo, J., Su, Z., and Huang, R. (1998). Two-kidney, two clip renovascular hypertensive rats can be used as stroke-prone rats. Stroke 29(8), 1708–1713; discussion 1713–1704.

Zhou, J., Ando, H., Macova, M., Dou, J., and Saavedra, J.M. (2005). Angiotensin II AT1 receptor blockade abolishes brain microvascular inflammation and heat shock protein responses in hypertensive rats. J. Cereb. Blood Flow Metab. 25(7), 878–886.

Address correspondence to:
Raymond Tak-Fai Cheung, Ph.D.
Department of Medicine
Rm 805, Administrative Block
Queen Mary Hospital
102 Pokfulam Road
Hong Kong, China

E-mail: rtcheung@hku.hk